Decoy exosomes provide protection against bacterial toxins

https://doi.org/10.1038/s41586-020-2066-6

Received: 7 December 2018

Accepted: 9 January 2020

Published online: 4 March 2020

Check for updates

Matthew D. Keller[1,2], Krystal L. Ching[1,2], Feng-Xia Liang[3,4], Avantika Dhabaria[3,5], Kayan Tam[1], Beatrix M. Ueberheide[3,5,6], Derya Unutmaz[7], Victor J. Torres[1,9]✉ & Ken Cadwell[1,2,8,9]✉

The production of pore-forming toxins that disrupt the plasma membrane of host cells is a common virulence strategy for bacterial pathogens such as methicillin-resistant *Staphylococcus aureus* (MRSA)[1–3]. It is unclear, however, whether host species possess innate immune mechanisms that can neutralize pore-forming toxins during infection. We previously showed that the autophagy protein ATG16L1 is necessary for protection against MRSA strains encoding α-toxin[4]—a pore-forming toxin that binds the metalloprotease ADAM10 on the surface of a broad range of target cells and tissues[2,5,6]. Autophagy typically involves the targeting of cytosolic material to the lysosome for degradation. Here we demonstrate that ATG16L1 and other ATG proteins mediate protection against α-toxin through the release of ADAM10 on exosomes—extracellular vesicles of endosomal origin. Bacterial DNA and CpG DNA induce the secretion of ADAM10-bearing exosomes from human cells as well as in mice. Transferred exosomes protect host cells in vitro by serving as scavengers that can bind multiple toxins, and improve the survival of mice infected with MRSA in vivo. These findings indicate that ATG proteins mediate a previously unknown form of defence in response to infection, facilitating the release of exosomes that serve as decoys for bacterially produced toxins.

We previously demonstrated that primary cells obtained from mice with hypomorphic expression of *Atg16l1* (*Atg16l1*^{HM}) display an increase in total ADAM10 levels and are susceptible to lysis when cultured in the presence of α-toxin[4]. Consistent with these findings, we have now found that levels of cell-surface and total ADAM10 are increased in the human alveolar epithelial cell line A549 upon short hairpin (sh)RNA-mediated depletion of *ATG16L1* (Fig. 1a–d). *ATG16L1*-knockdown cells treated with purified α-toxin displayed increased cell death compared with control cells transduced with nontargeting shRNA, whereas *ADAM10*-knockdown cells were resistant (Fig. 1e). ATG16L1 mediates the conjugation of phosphatidylethanolamine to the ubiquitin-like molecule LC3—a step that is necessary for the proper biogenesis of the autophagosome and for subsequent events in which substrates are degraded by the lysosome[7]. Inhibiting ULK1, a kinase upstream of ATG16L1, or ATG5, a binding partner of ATG16L1, led to increased cell-surface ADAM10 levels similar to those produced by knocking down *ATG16L1* (Fig. 1f). Prevention of lysosomal acidification by weak bases alters endosomal recycling to the plasma membrane[8,9]. Although total levels of ADAM10 and the autophagy substrate SQSTM1 were increased when A549 cells were treated with lysosomal acidification inhibitors (NH_4Cl, chloroquine or bafilomycin), all three agents decreased surface ADAM10 levels (Fig. 1g, h and Extended Data Fig. 1a–d). Surface levels of epithelial cell adhesion molecule (EpCAM) were unaltered, indicating that lysosome inhibition did not affect all plasma-membrane molecules (Extended Data Fig. 1e–g). ADAM10 levels were unaffected by proteasome inhibition (Extended Data Fig. 1h, i), suggesting that ATG proteins reduce cell-surface ADAM10 through a lysosome- and proteasome-independent process.

ATG proteins mediate the extracellular release of soluble and vesicle-bound substrates through a process broadly referred to as secretory autophagy[10]. ADAM10 is known to be incorporated into exosomes—extracellular vesicles typically 40–120 nm in diameter[11,12]. Thus, we hypothesized that the autophagy machinery prevents ADAM10 accumulation on cells by facilitating its secretion on exosomes. We found a reduction in the lower-molecular-weight band of ADAM10 (a mature form cleaved during trafficking from the endoplasmic reticulum) in exosome fractions isolated from the culture supernatants of *ATG16L1*-knockdown cells compared with control cells treated with nontargeting shRNA (Fig. 2a, b and Extended Data Fig. 2a). Western blot analysis confirmed that the fractionation procedure led to enrichment of the exosomal marker CD9 and not the microvesicle marker ARF6 (Extended Data Fig. 2b). Parallel analysis by transmission electron microscopy (TEM) indicated that the exosome fraction contained a greater number of single-lipid-bilayer vesicles of 80–150 nm in diameter compared with microvesicles larger than 150 nm (Extended Data Fig. 2c–e).

The decrease in ADAM10 that occurs after ATG16L1 inhibition reflects a general reduction in exosome levels: we observed a reduction in CD9 levels by western blot and a reduction in the number of vesicles by TEM

[1]Department of Microbiology, New York University School of Medicine, New York, NY, USA. [2]Kimmel Center for Biology and Medicine at the Skirball Institute, New York University School of Medicine, New York, NY, USA. [3]Division of Advanced Research Technologies, New York University Langone Health, New York, NY, USA. [4]The Microscopy Labratory at New York University Langone Health, New York, NY, USA. [5]The Proteomics Labratory at New York University Langone Health, New York, NY, USA. [6]The Laura and Isaac Perlmutter Cancer Center, New York, NY, USA. [7]Jackson Laboratory for Genomic Medicine, Farmington, CT, USA. [8]Division of Gastroenterology and Hepatology, Department of Medicine, New York University Langone Health, New York, NY, USA. [9]These authors contributed equally: Victor J. Torres, Ken Cadwell. ✉e-mail: Victor.Torres@nyulangone.org; Ken.Cadwell@nyulangone.org

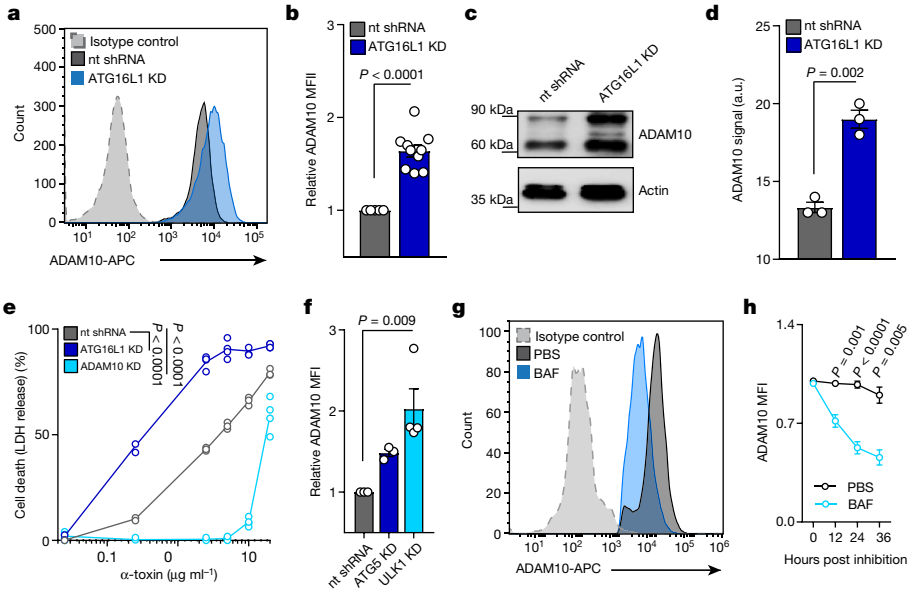

Fig. 1 | ATG16L1 inhibits surface ADAM10 independently of lysosomal degradation. a, **b**, Representative flow-cytometry histogram (**a**) and quantification of mean fluorescent intensity (MFI) (**b**) of surface ADAM10 in A459 cells following *ATG16L1* knockdown (ATG16L1 KD; $n = 5$); or in cells containing nontargeting control shRNA (nt shRNA; $n = 10$). **c**, **d**, Representative western blot (**c**) and quantification (**d**) of ADAM10 in ATG16L1 KD and control cells; $n = 3$. a.u., arbitrary units. **e**, Quantification of cell death (assayed by release of lactate dehydrogenase, LDH) of nt shRNA, ATG16L1 KD and ADAM10 KD cells following treatment with purified α-toxin; $n = 4$. **f**, Quantification of surface ADAM10 by flow cytometry in nt shRNA ($n = 3$), ATG5 KD ($n = 3$) and ULK1 KD ($n = 4$) A549 cells. **g**, **h**, Representative flow-cytometry histogram from three independent repeats of surface ADAM10 on A549 cells 24 h after treatment with bafilomycin (BAF; 10 nM) (**g**), and quantification of MFI over time following addition of BAF (**h**; $n = 3$). PBS, phosphate-buffered saline. Measurements were taken from distinct samples, and graphs show means and standard errors of the mean (s.e.m.). **b**, **d**, **f**, **h**, Two-tailed, unpaired *t*-test with Welch's correction compared with nt shRNA controls. **e**, Two-tailed, unpaired *t*-test of area under curve compared with nt shRNA controls.

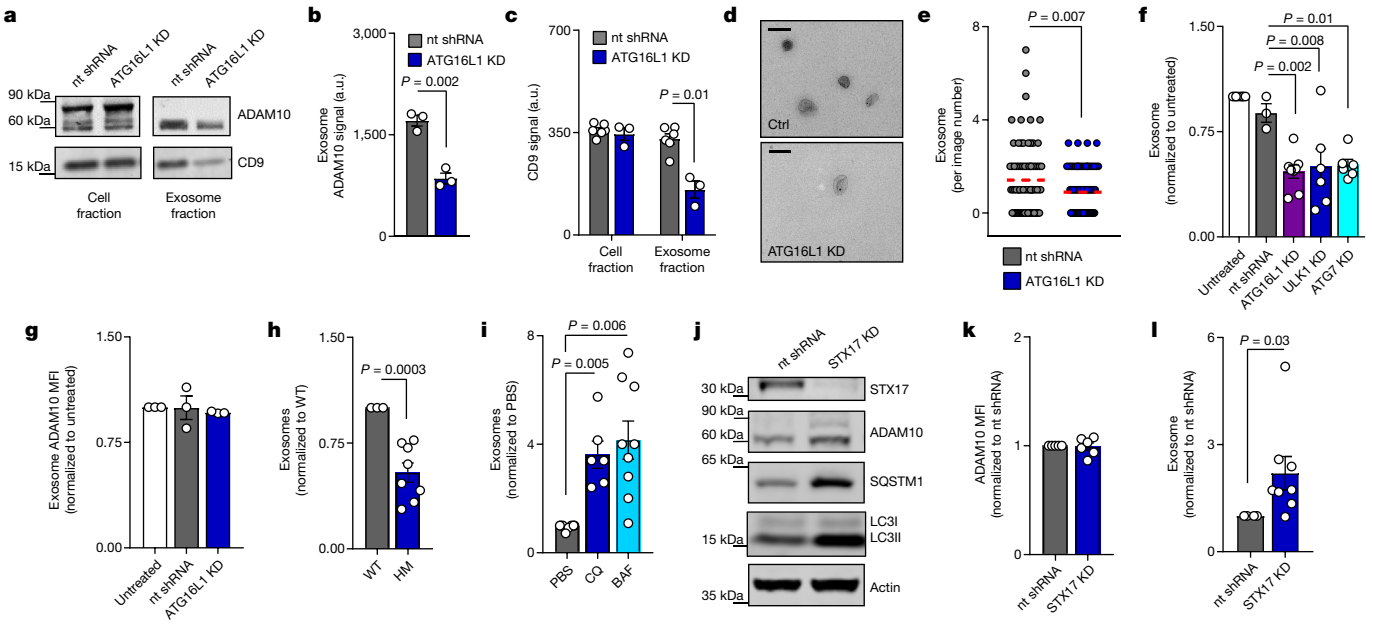

Fig. 2 | ATG proteins regulate the release of ADAM10-containing exosomes. **a**–**c**, Representative ADAM10 and CD9 western blot from three independently repeated experiments (**a**); quantification of exosome ADAM10, $n = 3$ (**b**); and quantification of CD9 in cell lysates and exosomes from nt shRNA ($n = 7$) and ATG16L1 KD ($n = 3$) cells (**c**). **d**, **e**, Representative transmission electron micrographs (**d**) and quantification (**e**) of vesicles in the exosome fraction of nt shRNA and ATG16L1 KD culture supernatants. Scale bars, 100 μm; $n = 80$ images. Ctrl, control. **f**, Flow-cytometric quantification of exosomes from untreated ($n = 4$), nt shRNA ($n = 3$), ATG16L1 KD ($n = 7$), ULK1 KD ($n = 6$) and ATG7 KD ($n = 6$) A549 cells. **g**, Quantification of ADAM10 MFI in untreated, nt shRNA and ATG16L1 KD exosomes from **f**. $n = 3$. **h**, Exosome quantification ($CD9^+$, $CD63^+$, $CD81^+$ and $PKH67^+$ structures) in blood from C57BL/6J (wild-type (WT); $n = 6$) and ATG16L1 hypomorph (HM; $n = 8$) mice. **i**, Exosome quantification following addition of PBS ($n = 4$), chloroquine (CQ; $n = 5$) or BAF ($n = 9$). **j**, Representative western blot from three independent repeats analysing ADAM10, SQSTM1 and LC3II levels in nt shRNA and STX17 KD cells. **k**, ADAM10 MFI of nt shRNA ($n = 5$) and STX17 KD ($n = 6$) cells. **l**, Exosome quantification from nt shRNA and STX17 KD cells; $n = 8$. Measurements were taken from distinct samples and graphs show means ± s.e.m. **b**, **c**, **e**, **h**, **l**, Two-tailed, unpaired *t*-test with Welch's correction compared with nt shRNA or WT controls. **f**, **g**, **i**, One-way analysis of variance (ANOVA) with Dunnet's post-test compared with nt shRNA or PBS. Data represent at least three independent experiments.

in the exosome fraction of *ATG16L1*-knockdown cell-culture supernatant (Fig. 2a, c–e). To further validate these results through a quantitative assay, we used flow cytometry in which antibody-based staining of the surface exosome markers CD9, CD63 and CD81 was combined with PKH67, a fluorescent lipid-bilayer-intercalating compound (Extended Data Fig. 2f). Depletion of autophagy proteins substantially reduced the total numbers of exosomes in the culture supernatant (Fig. 2f). *ATG16L1*-knockdown reduced the total number of ADAM10-positive exosomes but not the amount of ADAM10 per exosome (Fig. 2g), confirming that the ATG proteins regulate exosome biogenesis rather than substrate incorporation. We also found that the blood from *Atg16l1*^{HM} mice contained fewer exosomes than blood from wild-type mice (Fig. 2h).

Our finding that blocking lysosomal acidification decreases plasma-membrane ADAM10 levels could be explained by a mechanism in which inhibiting late-stage autophagy redirects the autophagy machinery towards generation of exosomes[13–15]. Consistent with this possibility, we detected increases in CD9 and ADAM10 levels in the exosome fraction as well as an increase in total exosome numbers in the culture supernatant of cells treated with chloroquine or bafilomycin (Fig. 2i and Extended Data Fig. 3a–d). The SNARE protein syntaxin 17 (STX17) mediates autophagosome–lysosome fusion and is dispensable for secretory autophagy[16,17]. *STX17* knockdown increased total ADAM10, SQSTM1 and LC3II levels, indicating successful inhibition of autophagy, without increasing surface levels of ADAM10 (Fig. 2j, k). However, supernatants from *STX17*-knockdown cells contained more exosomes (Fig. 2l), indicating that ATG proteins mediate the release of exosomes in a manner distinct from conventional degradative autophagy.

We next examined whether ATG-dependent exosome production is induced by pathogen exposure. Heat-killed *S. aureus* (CA-MRSA USA300, hereafter HKSA), an isogenic α-toxin-deficient USA300 strain (Δ*hla*), *Streptococcus pneumoniae*, *Citrobacter rodentium* and *Salmonella enterica* Typhimurium all increased exosome production in human and mouse cells (Fig. 3a and Extended Data Fig. 4a, i). After testing several bacterially derived products, we indentified bacterial DNA and CpG DNA as the exosome inducer (Fig. 3b and Extended Data Fig. 4b–g). Furthermore, addition of DNA isolated from *S. aureus* to cells elicited exosomes, and DNase treatment abolished this effect (Extended Data Fig. 4j). Exosome production in response to HKSA and CpG DNA depended on the endosomal DNA-sensor Toll-like receptor 9 (TLR9) (Fig. 3c and Extended Data Fig. 4h). Inducing autophagy with Torin-1—an inhibitor of mammalian target of rapamycin (mTOR)—did not induce exosomes, suggesting that TLR9 acts through a distinct mechanism (Extended Data Fig. 4k, l). Instead, the addition of CpG DNA or bafilomycin (a positive control) individually or together decreased LysoSensor staining, an indicator of acidic organelles (Extended Data Fig. 5a–c). We also found that treating cells with the neutral sphingomyelinase inhibitor GW4869—which prevents the generation of vesicles that become exosomes by interfering with the inward budding of the multivesicular body (MVB)[18]—impairs CpG-DNA-induced exosome production (Extended Data Fig. 4m). Thus, the membrane-trafficking events downstream of TLR9 probably contribute to exosome production by regulating endosomal trafficking and vesicle-biogenesis events that include the MVB.

Intravenous injection of heat-killed or live *S. aureus* into wild-type mice led to a marked increase in the number of exosomes in their blood that was blunted in *Atg16l1*^{HM} mice, but not in mice in which *Atg16l1* was selectively deleted in macrophage and dendritic-cell lineages (Fig. 3d, e and Extended Data Fig. 4n, o). This observation is consistent with our previous study in which *Atg16l1*^{HM} mice, but not myeloid-cell-specific *Atg16l1* knockout mice, were susceptible to lethal bloodstream infection by MRSA[4]. Next, we performed mass spectrometry on exosomes from the blood of mice inoculated intranasally with HKSA or CpG DNA (Extended Data Fig. 4p). The majority of detected proteins originated from the liver and were previously identified in exosomes and extracellular spaces (Fig. 3f–h and Supplementary Tables 1–3). We confirmed that the liver

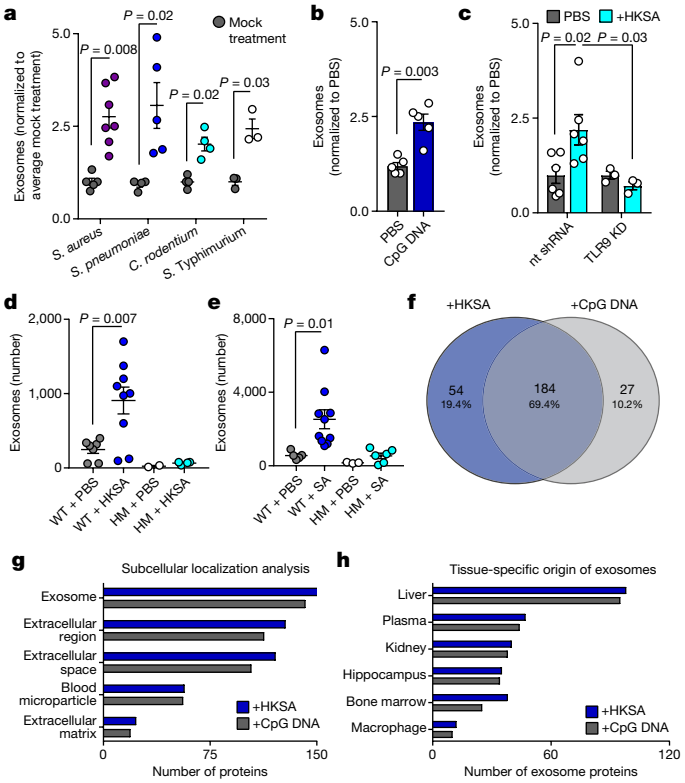

Fig. 3 | Bacteria induce exosome production. a–e, Flow-cytometric quantification of exosomes in A549 cell-culture supernatant 18 h after exposure to heat-killed *S. aureus* ($n = 7$), heat-killed *S. pneumoniae* ($n = 5$), heat-killed *C. rodentium* ($n = 4$), heat-killed *S.* Typhimurium ($n = 3$) (**a**); after CpG DNA treatment (4 μM; $n = 5$) (**b**); in nt shRNA ($n = 6$) and TLR9 shRNA (TLR9 KD; $n = 3$) targeted A549 cells following HKSA exposure (**c**); in blood from wild-type and *Atg16l1*^{HM} mice following intranasal (i.n.) inoculation with HKSA (1×10^8 colony-forming units (CFU); WT plus PBS, $n = 7$; WT plus HKSA, $n = 9$; HM plus PBS, $n = 2$; HM plus HKSA, $n = 4$) (**d**); or following intravenous (i.v.) inoculation with live *S. aureus* (1×10^7 CFU; WT plus PBS, $n = 5$; WT plus HKSA, $n = 10$; HM plus PBS, $n = 3$; HM plus HKSA, $n = 6$) (**e**). **f**, Venn diagram of shared and discreet proteins identified by mass spectrometry in exosomes isolated from the blood of mice exposed to HKSA or CpG DNA i.n. (1×10^8 CFU; 20 μg CpG DNA). **g**, Gene-ontology analysis of the subcellular location of proteins identified by mass spectrometry. **h**, Tissue-specific origin of exosome proteins. Measurements were taken from distinct samples and graphs show means ± s.e.m. **a**, **b**, Two-tailed, unpaired *t*-test with Welch's correction compared with PBS controls. **c–e**, One-way ANOVA with Dunnet's post-test compared with nt shRNA plus PBS, or WT plus PBS controls.

enzyme argininosuccinate synthase 1 (ASS1) was enriched in HKSA, and that CpG DNA elicited exosomes in vivo[19] (Extended Data Fig. 4p).

Next, we tested whether these released vesicles could serve as a host response to bind and inhibit toxins. We found that exosomes isolated from control donor cells, but not from *ATG16L1*-knockdown cells, were able to protect A549 target cells from α-toxin toxicity (Fig. 4a). Adding twice the volume of the supernatant of *ATG16L1*-knockdown cells from which exosomes were isolated improved the viability of the cells, indicating that the inability of exosomes from *ATG16L1*-knockdown cells to protect cells was due to a reduction in the number of exosomes. Exosomes harvested from *ADAM10*-knockdown cells were unable to protect cells (Fig. 4a and Extended Data Fig. 6a). These results were confirmed with exosomes purified through fluorescence-activated cell sorting (FACS; Fig. 4b). Of note, preincubating cells with HKSA or CpG DNA also protected against α-toxin toxicity (Extended Data Fig. 6b). This protection was due to exosomes: removing the exosome-containing supernatant restored susceptibility to α-toxin in HKSA

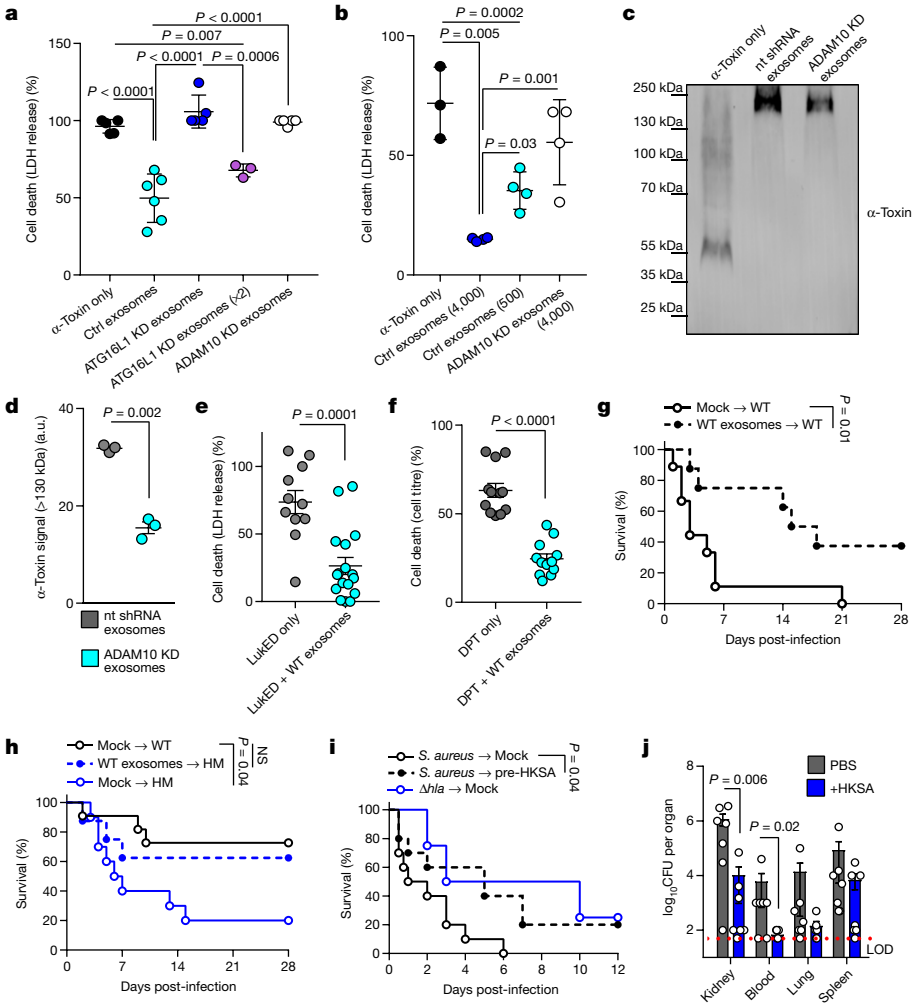

Fig. 4 | Exosomes protect against bacterial toxins. a, **b**, A549 cell death following treatment with α-toxin together with exosomes isolated from nt shRNA ($n = 6$), ATG16L1 KD ($n = 6$), ATG16L1 KD × 2 ($n = 3$), ADAM10 KD ($n = 5$) cells (**a**); or with FACS-purified exosomes ($n = 4$) (**b**). **c**, **d**, Representative western blot (**c**) and quantification (**d**) of oligomerized α-toxin larger than 130 kDa following addition of exosomes isolated from WT or ADAM10 KD cells. $n = 3$. **e**, BMDM death following treatment with LukED and exosomes isolated from WT BMDM cultures (LukED only, $n = 10$; LukED plus WT exosomes, $n = 16$). **f**, A549 cell death following exposure to diphtheria toxin (DPT) and exosomes isolated from A549 cultures. $n = 12$. **g**, Survival of WT mice infected i.v. with *S. aureus* (USA300; 5×10^7 CFU) mock-treated or injected intraperitoneally with exosomes from WT mice. $n = 9$ mice per condition. **h**, Survival of WT ($n = 10$) and *Atg16l1*^{HM} (Mock to HM, $n = 10$; WT exosomes to HM, $n = 10$) mice infected i.v. with 2.5×10^7 CFU of *S. aureus* and receiving exosomes from WT mice. NS, not significant. **i**, Survival of WT mice ($n = 10$) pretreated with intranasal HKSA followed by a lethal dose of *S. aureus* (strain USA300; 5×10^7 CFU; $n = 10$) or an isogenic α-toxin-deficient strain (Δ*hla*; $n = 5$). **j**, *S. aureus* burden 24 h after infection with 1×10^7 CFU of USA300 i.v. in kidney, spleen, lung and blood (per millilitre) in mice pretreated with PBS or HKSA i.v.; $n = 6$. Measurements were taken from distinct samples. LOD, limit of detection. Graphs show means ± s.e.m. **a**, **b**, One-way ANOVA with Dunnet's post-test compared with α-toxin only or control exosomes. **d**–**f**, **j**, Two-tailed, unpaired *t*-test with Welch's correction compared with nt shRNA exosomes, α-toxin only or PBS controls. **g**–**i**, log-rank Mantel–Cox test.

or CpG-DNA-treated cells (Extended Data Fig. 6b). Exosomes seem to protect cells by inducing toxin oligomerization on the exosome membranes (Fig. 4c, d).

Exosomes elicited from mouse bone-marrow-derived macrophages (BMDMs) harbour the toxin receptor CCR5 and protected BMDMs from LukED (Fig. 4e and Extended Data Fig. 6c), another toxin produced by *S. aureus*[20]. Similarly, exosomes isolated from A549 cells protected target cells from diphtheria toxin (Fig. 4f), a potent toxin produced by *Corynebacterium diphtheriae* that binds to the epidermal growth factor receptor (EGFR)[21], which was present in our exosome proteomics dataset (Supplementary Table 1). Thus, exosomes can neutralize different types of toxin.

To test whether exosomes are protective in vivo, we injected donor mice with HKSA to elicit exosomes in the blood; we then transferred these exosomes into recipient mice and infected the animals intravenously with a lethal dose of *S. aureus*. Transfer of exosomes from wild-type but not *Atg16l1*^{HM} donors extended the survival of *S. aureus*-infected wild-type recipient mice (Fig. 4g and Extended Data Fig. 6d, e). Furthermore, transfer of exosomes from a wild-type donor improved the survival of *Atg16l1*^{HM} mice injected with lethal dose 50 of *S. aureus* to levels similar to those of mock-treated wild-type mice (Fig. 4h), suggesting that the increased susceptibility of *Atg16l1* mutants is in part due to reduced exosome production.

Finally, priming mice with intravenous injection of HKSA increased the relative amount of α-toxin oligomers to monomers in the exosome fraction isolated from the bronchoalveolar lavage (BAL) fluid compared with mock-treated controls (Extended Data Fig. 6f–k). Additionally, we found that conditioning the mice with HKSA prolonged survival following *S. aureus* infection, phenocopying control mice infected with the Δ*hla* strain (Fig. 4i). To monitor bacterial burden, we challenged mice with a lower inoculum, and found that conditioning with HKSA resulted in reduction in *S. aureus* burdens in the kidneys and blood (Fig. 4j).

Exosomes extend the functional reach of their cells of origin and contribute to a spectrum of biological processes[22,23]. Our results suggest that exosomes can also provide a previously undescribed innate immune response to bacterial infection by acting as decoys that trap membrane-acting virulence factors, such as pore-forming toxins, to prevent injury of target tissues. The action of these 'defensosomes' is in line with recent evidence that engineered liposomes can neutralize toxins from Gram-positive bacteria[24]. Our findings also indicate that ATG proteins regulate the production of exosomes during host defence—a mechanism that is distinct from the recently uncovered roles of ATG16L1 in promoting plasma-membrane repair during *Listeria monocytogenes* infection, or in preventing necroptosis mediated by the pore-forming molecule MLKL during norovirus infection[25,26]. Rather, our findings resemble recently described processes in which extracellular vesicles are produced when the atypical ATG12–ATG3 conjugate promotes MVB function, or when ATG5 disrupts lysosomal acidification[27,28]. Given that the origin and regulation of extracellular vesicles remain poorly defined, a detailed understanding of the cellular response triggering the production of defensosomes during infection may reveal opportunities to leverage their unique properties to combat bacteria and other pathogens.

Online content

Any methods, additional references, Nature Research reporting summaries, source data, extended data, supplementary information, acknowledgements, peer review information; details of author contributions and competing interests; and statements of data and code availability are available at https://doi.org/10.1038/s41586-020-2066-6.

1. Dal Peraro, M. & van der Goot, F. G. Pore-forming toxins: ancient, but never really out of fashion. *Nat. Rev. Microbiol.* **14**, 77–92 (2016).
2. Seilie, E. S. & Bubeck Wardenburg, J. *Staphylococcus aureus* pore-forming toxins: the interface of pathogen and host complexity. *Semin. Cell Dev. Biol.* **72**, 101–116 (2017).
3. Spaan, A. N., van Strijp, J. A. G. & Torres, V. J. Leukocidins: staphylococcal bi-component pore-forming toxins find their receptors. *Nat. Rev. Microbiol.* **15**, 435–447 (2017).
4. Maurer, K. et al. Autophagy mediates tolerance to *Staphylococcus aureus* alpha-toxin. *Cell Host Microbe* **17**, 429–440 (2015).
5. Inoshima, I. et al. A *Staphylococcus aureus* pore-forming toxin subverts the activity of ADAM10 to cause lethal infection in mice. *Nat. Med.* **17**, 1310–1314 (2011).
6. Becker, R. E., Berube, B. J., Sampedro, G. R., DeDent, A. C. & Bubeck Wardenburg, J. Tissue-specific patterning of host innate immune responses by *Staphylococcus aureus* α-toxin. *J. Innate Immun.* **6**, 619–631 (2014).
7. Matsuzawa-Ishimoto, Y., Hwang, S. & Cadwell, K. Autophagy and inflammation. *Annu. Rev. Immunol.* **36**, 73–101 (2018).
8. Presley, J. F., Mayor, S., McGraw, T. E., Dunn, K. W. & Maxfield, F. R. Bafilomycin A1 treatment retards transferrin receptor recycling more than bulk membrane recycling. **272**, 13929–13936 (1997).
9. Johnson, L. S., Dunn, K. W., Pytowski, B. & McGraw, T. E. Endosome acidification and receptor trafficking: bafilomycin A1 slows receptor externalization by a mechanism involving the receptor's internalization motif. **4**, 1251–1266 (1993).
10. Cadwell, K. & Debnath, J. Beyond self-eating: the control of nonautophagic functions and signaling pathways by autophagy-related proteins. *J. Cell Biol.* **217**, 813–822 (2018).
11. Stoeck, A. et al. A role for exosomes in the constitutive and stimulus-induced ectodomain cleavage of L1 and CD44. *Biochem. J.* **393**, 609–618 (2006).
12. Shimoda, M. et al. Loss of the Timp gene family is sufficient for the acquisition of the CAF-like cell state. *Nat. Cell Biol.* **16**, 889–901 (2014).
13. Ejlerskov, P. et al. Tubulin polymerization-promoting protein (TPPP/p25α) promotes unconventional secretion of α-synuclein through exophagy by impairing autophagosome-lysosome fusion. *J. Biol. Chem.* **288**, 17313–17335 (2013).
14. Guo, H. et al. Atg5 disassociates the V1V0-ATPase to promote exosome production and tumor metastasis independent of canonical macroautophagy. *Dev. Cell* **43**, 716–730 (2017).
15. Miao, Y., Li, G., Zhang, X., Xu, H. & Abraham, S. N. A TRP channel senses lysosome neutralization by pathogens to trigger their expulsion. *Cell* **161**, 1306–1319 (2015).
16. Itakura, E., Kishi-Itakura, C. & Mizushima, N. The hairpin-type tail-anchored SNARE syntaxin 17 targets to autophagosomes for fusion with endosomes/lysosomes. *Cell* **151**, 1256–1269 (2012).
17. Kimura, T. et al. Dedicated SNAREs and specialized TRIM cargo receptors mediate secretory autophagy. *EMBO J.* **36**, 42–60 (2017).
18. Trajkovic, K. et al. Ceramide triggers budding of exosome vesicles into multivesicular endosomes. *Science* **319**, 1244–1247 (2008).
19. Cho, Y. E. et al. Increased liver-specific proteins in circulating extracellular vesicles as potential biomarkers for drug- and alcohol-induced liver injury. *PLoS One* **12**, e0172463 (2017).
20. Alonzo, F., III et al. CCR5 is a receptor for *Staphylococcus aureus* leukotoxin ED. *Nature* **493**, 51–55 (2013).
21. Mitamura, T., Higashiyama, S., Taniguchi, N., Klagsbrun, M. & Mekada, E. Diphtheria toxin binds to the epidermal growth factor (EGF)-like domain of human heparin-binding EGF-like growth factor/diphtheria toxin receptor and inhibits specifically its mitogenic activity. *J. Biol. Chem.* **270**, 1015–1019 (1995).
22. Montecalvo, A. et al. Mechanism of transfer of functional microRNAs between mouse dendritic cells via exosomes. *Blood* **119**, 756–766 (2012).
23. Kalluri, R. The biology and function of exosomes in cancer. *J. Clin. Invest.* **126**, 1208–1215 (2016).
24. Henry, B. D. et al. Engineered liposomes sequester bacterial exotoxins and protect from severe invasive infections in mice. *Nat. Biotechnol.* **33**, 81–88 (2015).
25. Tan, J. M. J. et al. An ATG16L1-dependent pathway promotes plasma membrane repair and limits *Listeria monocytogenes* cell-to-cell spread. *Nat. Microbiol.* **3**, 1472–1485 (2018).
26. Matsuzawa-Ishimoto, Y. et al. Autophagy protein ATG16L1 prevents necroptosis in the intestinal epithelium. *J. Exp. Med.* **214**, 3687–3705 (2017).
27. Murrow, L., Malhotra, R. & Debnath, J. ATG12–ATG3 interacts with Alix to promote basal autophagic flux and late endosome function. *Nat. Cell Biol.* **17**, 300–310 (2015).
28. Guo, H. et al. Atg5 disassociates the V_1V_0-ATPase to promote exosome production and tumor metastasis independent of canonical macroautophagy. *Dev. Cell* **43**, 716–730 (2017).

Methods

Mice

Age- and gender-matched 8–12-week-old mice on the C57BL/6J background were used. *Atg16L1*^{HM} mice on the C57BL/6J background were previously described[4,29,30]. 'Wild-type' refers to littermate controls generated from breeder pairs that were heterozygous for the *Atg16L1*^{HM} allele for experiments that involve comparisons between genotype. For other experiments, C57BL/6J mice were purchased from the Jackson Laboratory and bred onsite. All animal studies were performed according to approved protocols and ethical guidelines established by the NYU School of Medicine Institutional Animal Care and Use Committee (IACUC) and Institutional Review Board.

Cell lines

For in vitro studies, the human lung epithelial cell line, A549, was purchased from ATCC (catalogue number CCL-185). Human embryonal kidney cells, HEK293FT, purchased from ThermoFisher (catalogue number R70007), were used for lentiviral packaging. All cell lines were confirmed as free from mycoplasma contamination.

Bacterial growth

S. aureus strain LAC/USA300 was grown overnight in tryptic soy broth (TSB) with shaking at 37 °C and diluted 1/100 followed by an additional 3–4 h of growth until bacteria reached an optical density of 2. *S. pneumoniae* strain D39 was grown overnight in Luria–Bertani (LB) broth at 37 °C. The following day *S. pneumoniae* was diluted 1/50 followed by 4 h of growth until the optical density reached 0.5. *C. rodentium* and *S.* Typhimurium were grown overnight in LB broth at 37 °C. The following day, both were diluted 1/10 followed by 4 h of growth until the optical density reached 2.0. Bacterial density was confirmed by dilution plating. 1×10^9 CFU of each bacterial strain were boiled at 95 °C for 2 h and resuspended in PBS for experiments with heat-killed bacteria.

shRNA knockdown

Lentivirus-based knockdown of human *ATG16L1* (5′-CCGGACTG TAGCTTTGCCGTGAATGCTCGAGCATTCACGGCAAAGCTACAGTTTTT TTG-3′), *ULK1* (5′-CCGGGCCCTTTGCGTTATATTGTATCTCGAGATA CAATATAACGCAAAGGGCTTTTT-3′), *ATG5* (5′-CCGGGATTCATGGA ATTGAGCCAATCTCGAGATTGGCTCAATTCCATGAATCTTTTTTG-3′), *ATG7* (5′-CCGGGCTTTGGGATTTGACACATTTCTCGAGAAATGTGTC AAATCCCAAAGCTTTTT-3′), *ADAM10* (5′-CCGGCCAGGTGGAATTACTTA ATTCTCGAAGAATTTAAGTAATTCCTGGTTTTT-3′) and nontargeting control were performed using MISSION shRNA constructs (Sigma-Aldrich) as described[31]. Viruses expressing shRNAs were produced by DNA transfection via Lipofectamine 3000 (ThermoFisher). Successful knockdown was confirmed by western blot and/or reverse transcription (RT) with quantitative polymerase chain reaction (qPCR).

Flow cytometry

A549 cells were stained for surface markers ADAM10 (human SHM14) and EpCAM (human 9C4) using antibodies from BioLegend. A fixable live/dead stain from BioLegend was used to exclude dead cells. For profiling, exosome pellets were resuspended in 100 µl of PBS and were stained with a combination of CD9 (human Hl9a, mouse MZ3), CD63 (human H5C6, mouse NVG-2), CD81 (human 5a6, mouse Eat-2), CCR5 (mouse HM-CCR5) and/or ADAM10 surface antibodies from BioLegend for 60 min at 4 °C. Exosome fractions were then stained with PKH67 (Sigma) as recommended by the manufacturer. Exosome fractions were washed in 40 ml PBS and ultracentrifuged again at 100,000*g* for 60 min. Washed exosome pellets were resuspended PBS. For LysoSensor experiments, A549 cells were stimulated for 4 h (1 µM CpG-A, 10 nM bafilomycin, or medium alone). Cells were loaded with 1 µM Lysosensor Green DND-189 (Molecular Probes, Invitrogen) diluted in prewarmed medium and incubated for 15 min at 37 °C. Cells were collected with 1 ml 5 mM PBS-EDTA and washed once with FACS buffer (5% FCS, 1× PBS, 2 mM EDTA). Cells and exosomes were analysed using Beckman Coulter Cytoflex Cytometer. For FACS-assisted purification, exosome identification and isolation were performed as described[32], and stained with a combination of CD81, CD63 and PHK67. Exosomes were sorted using the FACS ARIA IIu SORP cell sorter.

Western blotting

We collected 1×10^6 cells, washed them with PBS, and suspended them in RIPA buffer (Thermo-Scientific) containing 10× protease inhibitor (Santa Cruz Biotechnologies). Tissue homogenate was then pelleted twice at 10,000*g* for 10 min at 4 °C. Protein concentration in the supernatant was measured by Bradford assay and reduced using 4× Laemmli buffer containing β-mercaptoethanol at 95 °C for 5 min. For gel electrophoresis, 10–30 µg of protein was run at 120 V for 1 h using a 4–12% gradient protein gel (Thermo Fisher). Proteins were then transferred to an Immuno-Blot polyvinylidene fluoride (PVDF) membrane through Bio-Rad semi-dry transfer apparatus for 1 h, at 12 V constant. Membrane was incubated for 30 min with 5% non-fat dairy milk, and mouse anti-β-actin (Abcam) at 1/10,000, polyclonal rabbit anti-ADAM10 (Cell Signaling) at 1/2,500, mouse anti-ATG16L1 (MBL) at 1/1,000, monoclonal rabbit anti-CD9 (Cell Signaling) at 1/1,000, monoclonal mouse anti-CD81 (Cell Signaling) at 1/1,000, polyclonal rabbit anti-ARF6 (Cell Signaling) at 1/2,000, polyclonal rabbit anti-ASS1 (Abcam) at 1/1,000, polyclonal rabbit anti-HLA (Sigma) at 1/5,000, polyclonal rabbit anti-SQSTM1 (Cell Signaling) at 1/2,000, monoclonal rabbit anti-LC3 (Cell Signaling) at 1/2,000, or polyclonal rabbit anti-STX17 (Abcam) at 1/1,000 were probed overnight at 4 °C. Membranes were washed three times for 5 min and probed with secondary antibody rabbit-anti mouse LICOR IRDye 800CW and goat anti-rabbit LICOR IRDye 800CW 680 antibodies for 1 h at room temperature. After additional washing, protein was then detected with a LICOR Odyssey CLX imaging system.

Exosome isolation

Forty-eight hours before isolation, 1×10^7 A549 cells were plated in 150-mm tissue-culture dishes. At 24 h before isolation, approximately 35–40 ml of 10% Dulbecco's modified Eagle medium (DMEM: 10% fetal bovine serum (FBS), 1% nonessential amino acids and 1% penicillin/streptomycin) was removed, and fresh 10% DMEM without supplements was added to each dish. On the day of exosome isolation, medium from each plate was removed and centrifuged once at 500*g* for 10 min, then centrifuged once at 10,000*g* for 10 min. Supernatants were passed through a 0.22-µm filter and finally ultracentrifuged at 100,000*g* for 90 min. Following ultracentrifugation, supernatant was discarded. The pellet remaining after ultracentrifugation was collected and used for downstream analysis. When assessing by western blot, normalization was performed by controlling for the number of cells seeded onto the plate, and input loading was confirmed by probing CD9 in the depleted cell fractions. For exosome isolation from broncholear lavage (BAL), mice were killed and the trachea exposed. Using a 0.5-inch blunt-nose needle, 1 ml of PBS was flushed into the lungs and removed three times. The exosome-isolation protocol was then performed on the remaining BAL fraction as described above.

α-Toxin and exosome treatment of cultured cells

To determine cell sensitivity to α-toxin, we seeded 3×10^4 A549 cells in 96-well plates and allowed them to attach overnight. Various concentrations of α-toxin were then added and incubated together for 3 h at 37 °C. We collected 50 ml of supernatant and measured cell death, either by LDH release (which indicates pore formation; Promega CytoTox-One Kit) or by metabolic activity via CellTiter (Promega catalogue number G3582). Total cytolysis was calculated according to the manufacturer's instructions. For experiments in which the protective ability of exosomes was analysed, 3×10^4 A549 cells were seeded in 96-well plates and allowed to attach overnight. Exosome fractions

were isolated from 35 ml of A549 culture supernatant as described above. The exosome fraction was mixed with 1 μg ml^{-1} α-toxin in PBS. The exosome/α-toxin mixture was incubated at 37 °C for 30 min and then added to plated A549 cells.

Heat-killed bacteria, bacterial components and inhibitors

We seeded 5 × 10^6 A549 cells and allowed them to attach overnight. The following day, cells were washed with PBS and new medium was added, including 5 × 10^6 CFU of heat-killed *S. aureus*, 2 × 10^5 CFU of heat-killed *S. pneumoniae*, 5 × 10^6 CFU of heat-killed *C. rodentium*, 5 × 10^6 CFU of heat-killed *S.* Typhimurium, 250 μg ml^{-1} lipoteichoic acid (LTA, Sigma, catalogue number L2515), 1 μg ml^{-1} lipopolysaccharide (LPS, InvivoGen, catalogue number tlrl-3pelps), 10 μg ml^{-1} peptidoglycan (PDG, Sigma, catalogue number 77140), 2 μM CpG DNA, 0.5 μg ml^{-1} Pam2CSK (InvivoGen, catalogue number tlrl-pm2 s-1), 0.5 μg ml^{-1} Pam3CSK (InvivoGen, catalogue number tlrl-pms), 0.5 μg ml^{-1} *S. aureus* (SA) genomic DNA (gDNA, 0.5 μg ml^{-1}), 0.5 μg ml^{-1} *S. aureus* RNA, 2 μM GW4869 (Sigma, catalogue number D1692) or 200 nM Torin-1 (Tocris, catalogue number 4247). After 4 h or 18 h, supernatants were removed from cultures and exosomes were collected as described above. Exosomes were identified and quantified using the aforementioned flow-cytometry protocol.

Infection and exosome treatment of mice

Donor mice received an intranasal treatment of heat-killed *S. aureus* to induce exosome production. After 4–6 h, mice were bled submandibularly and plasma was collected. The exosome fraction was collected as described above for A549 cells. Recipient wild-type or *Atg16L1^{HM}* mice each received exosomes intraperitonially isolated from 1 ml of plasma on day −1, day 0, and day +1 of infection in a final volume of 1 ml of PBS. Mice were intravenously infected with USA300 *S. aureus* on day 0, and were monitored daily for signs of morbidity.

α-Toxin purification from *S. aureus*

Primers VJT1391 (5′-GGGGG-AAGCTT-gtttgatatggaactcctgaatttttcg-3′; the underlined sequence is the HindIII site) and VJT1395 (5′ GATAA-GCTAGC-tta-GTGGTGGTGGTGGTGG-atttgtcatttcttc-3′; the underlined sequence is the NheI site) were used to amplify the promoter region of *hla* followed by the *hla* gene and polyhistidine tag (6 × His tag) from the genomic DNA of *S. aureus* strain Newman by PCR. The PCR product was then cloned into the pOS1 plasmid using the HindIII and NheI restriction sites to generate the pOS1-phla-hla-6his plasmid. The purified plasmid was transformed into *Escherichia coli* DH5α competent cells, selected by ampicillin resistance (100 μg ml^{-1}) and confirmed by colony PCR and Sanger sequencing (Genewiz). The plasmid from a positive clone was purified and electroporated into *S. aureus* RN4220, selected by resistance to chloramphenicol (10 μg ml^{-1}); the plasmid purified from RN4220 was then electroporated into *S. aureus* Newman Δ*lukED* Δ*hlgACB::tet* Δ*lukAB::spec* Δ*hla::ermC* (ΔΔΔΔ) and selected for by resistance to chloramphenicol (10 μg ml^{-1}) resistance. For purification of His-tagged α-toxin, the *S. aureus* Newman ΔΔΔΔ strain harbouring the pOS1-phla-hla-6his plasmid (strain VJT 45.56) were grown overnight in 5 ml TSB (Fisher) supplemented with chloramphenicol (10 μg ml^{-1}) at 37 °C, shaking at 180 rpm, then subcultured the following day at a 1/100 dilution in TSB supplemented with chloramphenicol (10 μg ml^{-1}) and incubated for 5 h at 37 °C, shaking at 180 rpm. The cultures were centrifuged for 15 min at 6,000 rpm and 4 °C, and the supernatants were filter-sterilized through a 0.22-μm filter (Corning). The filtrates were incubated in the presence of a final concentration of 10 mM imidazole and nickel-nitrilotriacetic acid (Ni-NTA) agarose resin (Qiagen) equilibrated with 10 mM imidazole (Fisher) in 1× Tris-buffered saline (TBS; Cellgro) for 30 min at 4 °C while nutating. The filtrates were passed through a glass column by gravity filtration, then Ni-NTA-bound toxins were washed with 25 mM imidazole, followed by a secondary wash with 1× TBS. The Ni-NTA-bound toxins were eluted using 500 mM imidazole. The eluted toxins were dialysed into 10% glycerol in 1× TBS and filtered through a 0.22-μm filter before storage at −80 °C. When required, the toxins were concentrated using concentrator columns (Ultra-15 Centrifugal Filter Units 10,000 NMWL, 15-ml volume capacity; EMD Millipore Amicon) before measuring protein concentration using absorbance at 280 nm with a Nanodrop (Thermo Scientific) and Beer-Lambert's equation. We separated 2 μg of the purified proteins by SDS–PAGE at 90 V for 120 min, followed by Coomassie blue staining to confirm protein purity by visualization.

Sample preparation for mass spectrometry

Exosomes were lysed in 8 M urea containing 10% SDS. Lysed exosomes were reduced using dithiothreitol (5 μl of 0.2 M concentration) for 1 h at 55 °C. The reduced cysteines were subsequently alkylated with iodoacetamide (5 μl of 0.5 M) for 45 min in the dark at room temperature. Each sample was loaded onto S-trap microcolumns (Protifi) according to the manufacturer's instructions. In brief, 3 μl of 12% phosphoric acid and 165 μl of binding buffer (90% methanol, 100 mM triethylammonium bicarbonate (TEAB)) were added to each sample. Samples were loaded onto the S-trap columns and centrifuged at 4,000*g* for 30 s. After three washes, 20 μl of 50 mM TEAB and 1 μg of trypsin (1/50 ratio) were added to the trap and incubated at 47 °C for 1 h. Peptides were then eluted using 40% acetonitrile (ACN) in 0.5% acetic acid followed by 80% ACN in 0.5% acetic acid. Eluted peptides were dried and concentrated in a SpeedVac.

Liquid chromatography–tandem mass spectrometry analysis

We loaded 1 μg of each sample onto a trap column (Acclaim PepMap 100 pre-column, 75 μm × 2 cm, C18, 3 μm, 100 Å, Thermo Scientific) connected to an analytical column (EASY-Spray column, 50 μm × 75 μm ID, PepMap RSLC C18, 2 μm, 100 Å, Thermo Scientific) using the autosampler of an Easy nLC 1000 (Thermo Scientific) with solvent A consisting of 2% acetonitrile in 0.5% acetic acid and solvent B consisting of 80% acetonitrile in 0.5% acetic acid. The peptide mixture was gradient eluted into the Orbitrap QExactive HF-X Mass Spectrometer (Thermo Scientific) using the following gradient: 5–35% solvent B for 120 min, 35–45% solvent B for 10 min, and 45–100% solvent B for 20 min. The full scan was acquired with a resolution of 60,000 (at an *m*/*z* ratio of 200), a target value of 3 × 10^6 and a maximum ion time of 45 ms. Following each full mass-spectrometry (MS) scan, 20 data-dependent MS/MS spectra were acquired. These MS/MS spectra were collected with a resolution of 15,000, an AGC target of 1 × 10^5, a maximum ion time of 120 ms, one microscan, a 2 *m*/*z* isolation window, a fixed first mass of 150 *m*/*z*, a dynamic exclusion of 30 s, and a normalized collision energy of 27.

Analysis of mass-spectrometry data

All acquired MS/MS spectra were searched against the UniProt mouse reference database using Sequest HT within Proteome Discoverer 1.4 (Thermo Fisher Scientific). The parameters for searching MS/MS data were set as follows: precursor mass tolerance ±10 ppm, fragment mass tolerance ± 0.02 Da, digestion enzyme trypsin allowing two missed cleavages, fixed modification of carbamidomethyl on cysteine, variable modification of oxidation on methionine, and variable modification of deamidation on glutamine and asparagine. The results were filtered using a 1% peptide and protein false discovery rate searched against a decoy database and requiring proteins to have at least two unique peptides.

α-Toxin oligomerization assay

Exosomes were collected from A549 culture supernatants as described above. Exosome fractions were resuspended in 30 μl PBS. α-Toxin was added to exosome suspension at a concentration of 1 μg ml^{-1}. The exosome/α-toxin combination was then shaken at room temperature for 1 h. Following incubation, the exosome/α-toxin mixture was resuspended in 40 ml PBS and spun at 100,000*g* for 90 min to pellet exosomes with bound α-toxin and remove excess α-toxin. The exosome fraction was resuspended in RIPA buffer containing 4× Laemmli buffer

without β-mercaptoethanol. For gel electrophoresis, each sample (including an α-toxin-only lane) was run at 120 V for 1 h using a 4–20% tris-glycine gradient protein gel (Thermo Fisher). Proteins were then transferred to an Immuno-Blot PVDF membrane through Bio-Rad semi-dry transfer apparatus for 1 h at a constant voltage of 12 V. Membrane was incubated for 30 min with 5% non-fat dairy milk, and mouse anti-α-toxin (Sigma) at 1/5,000 was probed overnight at 4 °C. Membranes were washed three times for 5 min and probed with secondary antibody goat anti-rabbit LICOR IRDye 800CW 680 antibodies for 1 h at room temperature. After additional washing, protein was then detected with a LICOR Odyssey CLX imaging system.

Transmission electron microscopy

For analysis of exosome morphology, we placed 5 µl of isolated exosomes on glow-discharged carbon-coated 400-mesh copper/rhodium grids and stained the samples with 1% uranyl acetate aquous solution. For whole-mount immune-electron microscopy, we deposited 5 µl of 2%-paraformaldehyde-fixed exosomes on glow-discharged formvar-carbon-coated copper grids, and allowed the samples to adsorb for 20 min. After washing with PBS, the grids were incubated with 50 mM glycine/PBS for 5 min, blocked with 1% coldwater fish skin gelatin (Sigma) for 10 min, and incubated with primary antibodies (anti-TSG101, Abcam) in blocking solution for 2 h at room temperature. Following washing with PBS, gold-conjugated secondary antibodies (15 nm protein-A–gold, Cell Microscopy Center, University Medical Center Utrecht; 12-nm colloidal gold AffiniPure goat anti-rabbit IgG (H+L), Jackson ImmunoReasearch Laboratories) were applied in the blocking buffer for 1 h. After washing with PBS, the grids were fixed in 1% glutaraldehyde in PBS for 5 min, washed with water, contrasted and embedded in a mixture of 3% uranyl acetate and 2% methylcellulose at a ratio of 1/9. All stained grids were examined under a Philips CM-12 electron microscope and photographed with a Gatan (4kx2.7k) digital camera (Gatan, Pleasanton, CA)[33].

Statistical analysis

All analyses were performed with Graphpad Prism v.7. The numbers of animals or biological replicates used herein were estimated on the basis of a power analysis with the following assumptions: the standard deviation will be roughly 20% of the mean; *P* values will be less than 0.05 when the null hypothesis is false; and the effect size (Cohen's *d*) is between 1.0 and 2.0. The minimal number of mice required under these conditions ranges from 6 to 28 for in vivo experiments. We have also carefully chosen the indicated sample size on the basis of empirical evidence of what is necessary to interpret the data and statistical significance. A unpaired two-tailed *t*-test with Welch's correction was used to evaluate differences between two groups. One-way ANOVA with Dunnet's post-test analysis was performed to evaluate differences between groups of three or more. The log-rank Mantel–Cox test was used for comparison of mortality curves. No randomization or blinding was used in this study.

Reporting summary

Further information on research design is available in the Nature Research Reporting Summary linked to this paper.

Data availability

The datasets generated herein are available from the corresponding authors upon request. Western blot gel source data can be found in Supplementary Fig. 1. All identified proteins from mass-spectrometry experiments and thier accession identification codes are listed in Supplementary Tables 1–3. Source Data for Fig. 4 and Extended Data Fig. 6 are available with the paper.

29. Hubbard-Lucey, V. M. et al. Autophagy gene Atg16L1 prevents lethal T cell alloreactivity mediated by dendritic cells. *Immunity* **41**, 579–591 (2014).
30. Marchiando, A. M. et al. A deficiency in the autophagy gene Atg16L1 enhances resistance to enteric bacterial infection. *Cell Host Microbe* **14**, 216–224 (2013).
31. DuMont, A. L. et al. *Staphylococcus aureus* LukAB cytotoxin kills human neutrophils by targeting the CD11b subunit of the integrin Mac-1. *Proc. Natl Acad. Sci. USA* **110**, 10794–10799 (2013).
32. van der Vlist, E. J., Nolte-'t Hoen, E. N., Stoorvogel, W., Arkesteijn, G. J. & Wauben, M. H. Fluorescent labeling of nano-sized vesicles released by cells and subsequent quantitative and qualitative analysis by high-resolution flow cytometry. *Nat. Protocols* **7**, 1311–1326 (2012).
33. Théry, C., Amigorena, S., Raposo, G. & Clayton, A. Isolation and characterization of exosomes from cell culture supernatants and biological fluids. *Curr. Protoc. Cell Biol.* **30**, 3.22.21–3.22.29 (2006).

Acknowledgements We thank members of the Cadwell and Torres laboratory for constructive comments over the years, and particularly I. Irnov and E. Anderson for providing purified *S. aureus* DNA and assisting with the LukED protection experiments, respectively. This work was supported in part by US National Institute of Health (NIH) grants R01 AI121244 (to K.C. and V.J.T.); R01 HL123340, R01 DK093668, R01 DK103788, R01 AI130945 and R01 HL125816 (to K.C.); R01 AI099394 and R01 AI105129 (to V.J.T.); T32 AI007180 and F31 HL137304 (to M.D.K.); and pilot awards from the NYU CTSA grant UL1TR001445 from the National Center for Advancing Translational Sciences (NCATS) (to K.C.) and NYU Cancer Center grant P30CA016087 (to K.C.). Cell sorting/flow cytometry (NYU Langone Health's Cytometry and Cell Sorting Laboratory), mass spectrometry (The Proteomics Labratory at NYU Langone Health) and electron-microscopy studies (The Microscopy Labratory at NYU Langone Health) are supported in part by NYU Langone Health's Laura and Isaac Perlmutter Cancer Center Support (grant P30CA016087) from the National Cancer Institute Langone. This work was also supported by a Faculty Scholar grant from the Howard Hughes Medical Institute, the Merieux Institute, the Kenneth Rainin Foundation, the Crohn's & Colitis Foundation and the Stony Wold-Herbert Fund (all to K.C.). K.C. and V.J.T. are Burroughs Wellcome Fund Investigators in the Pathogenesis of Infectious Diseases.

Author contributions M.D.K., V.J.T. and K.C. formulated the original hypothesis and designed the study. M.D.K. preformed the experiments and analysed the data. K.L.C. provided assistance with experiments that examined vesicle-trafficking events downstream of TLR9 activation. F.-X.L. provided assistance with TEM, and A.D. and B.M.U. performed and assisted in the analysis of mass-spectrometry experiments. K.T. generated the construct to express α-toxin, and purified and characterized the toxin. D.U. provided essential reagents and insight into the shRNA transduction experiments. M.D.K, V.J.T. and K.C. wrote the manuscript. All authors commented on the manuscript, data and conclusions.

Competing interests V.J.T. is an inventor on patents and patent applications filed by NYU, which are currently under commercial license to Janssen Biotech. K.C. has consulted for, or received an honorarium from, Puretech Health, Genentech and AbbVie; has received research support from Puretech Health, Pacific Biosciences and Pfizer; and has a provisional patent, US Patent application number 15/625,934.

Additional information
Supplementary information is available for this paper at https://doi.org/10.1038/s41586-020-2066-6.
Correspondence and requests for materials should be addressed to V.J.T. or K.C.
Peer review information *Nature* thanks Ivan Dikic, Lora Hooper, Andreas Peschel, Philip Stahl and the other, anonymous, reviewer(s) for their contribution to the peer review of this work.
Reprints and permissions information is available at http://www.nature.com/reprints.

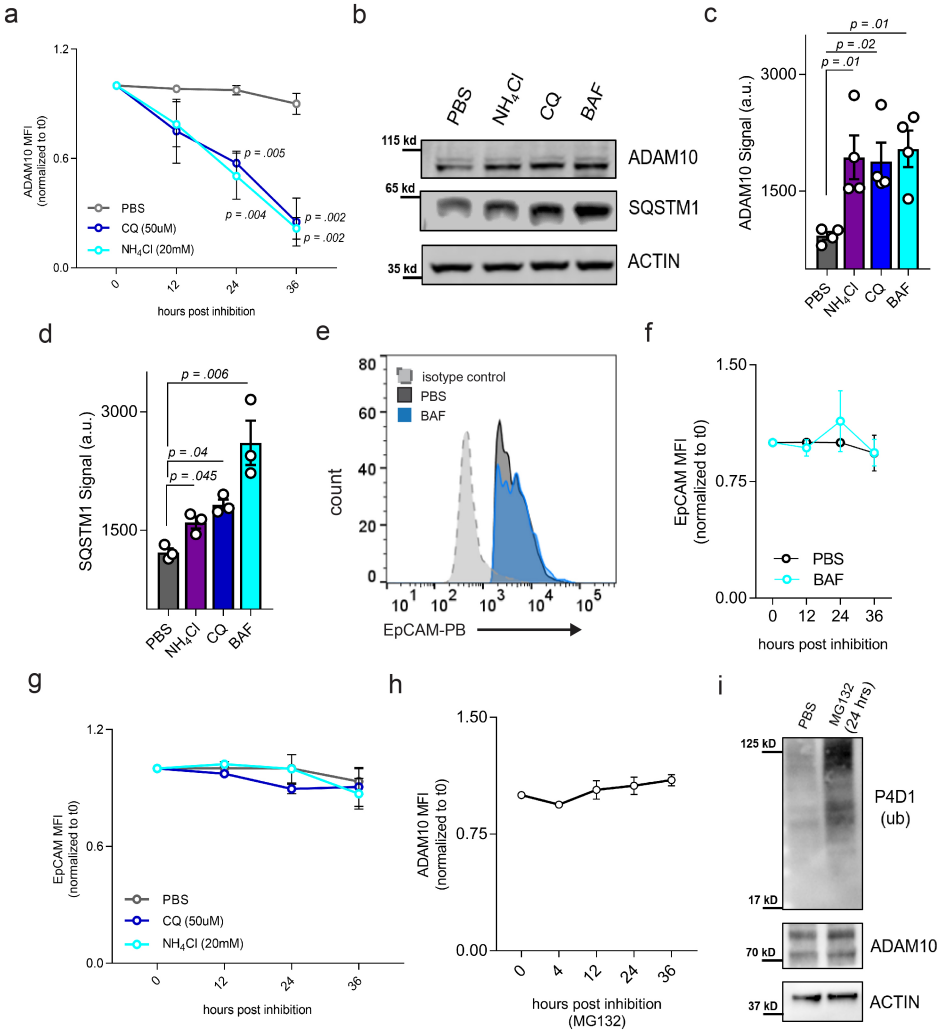

Extended Data Fig. 1 | ADAM10 and EpCAM levels following lysosomal inhibition with ammonium chloride, chloroquine or bafilomycin or proteasomal inhibition with MG132. a, Time course of flow-cytometry analysis of ADAM10 following lysosomal inhibition with ammonium chloride (NH_4Cl, 20 mM), chloroquine (CQ, 50 μM) or PBS as a control; $n = 3$. **b**–**d**, Western blot analysis of ADAM10 and SQSTM1 following lysosomal inhibition with NH_4Cl, CQ or bafilomycin (BAF, 10 nM). Shown are a representative western blot from four independent experiments (**b**), quantification of ADAM10 levels ($n = 5$) (**c**) and quantification of SQSTM1 levels ($n = 3$) (**d**) at 24 h after inhibition. **e**, **f**, Representative histogram (**e**) and quantification (**f**) of cell-surface EpCAM in BAF-treated A549 cells; $n = 3$. **g**, Time course of flow-cytometry analysis of EpCAM following treatment with NH_4Cl or CQ; $n = 4$. **h**, **i**, ADAM10, P4D1 and actin levels following proteasomal inhibition with the chemical compound MG132. Shown are a flow-cytometry time course of cell-surface ADAM10 levels following MG132 treatment (**h**) and a representative western blot from three independent experiments (**i**); $n = 3$. Measurements were taken from distinct samples and graphs show mean ± s.e.m. **a**, **c**, **d**, **f**–**h**, One-way ANOVA with Dunnet's post-test compared with PBS treatment or time 0.

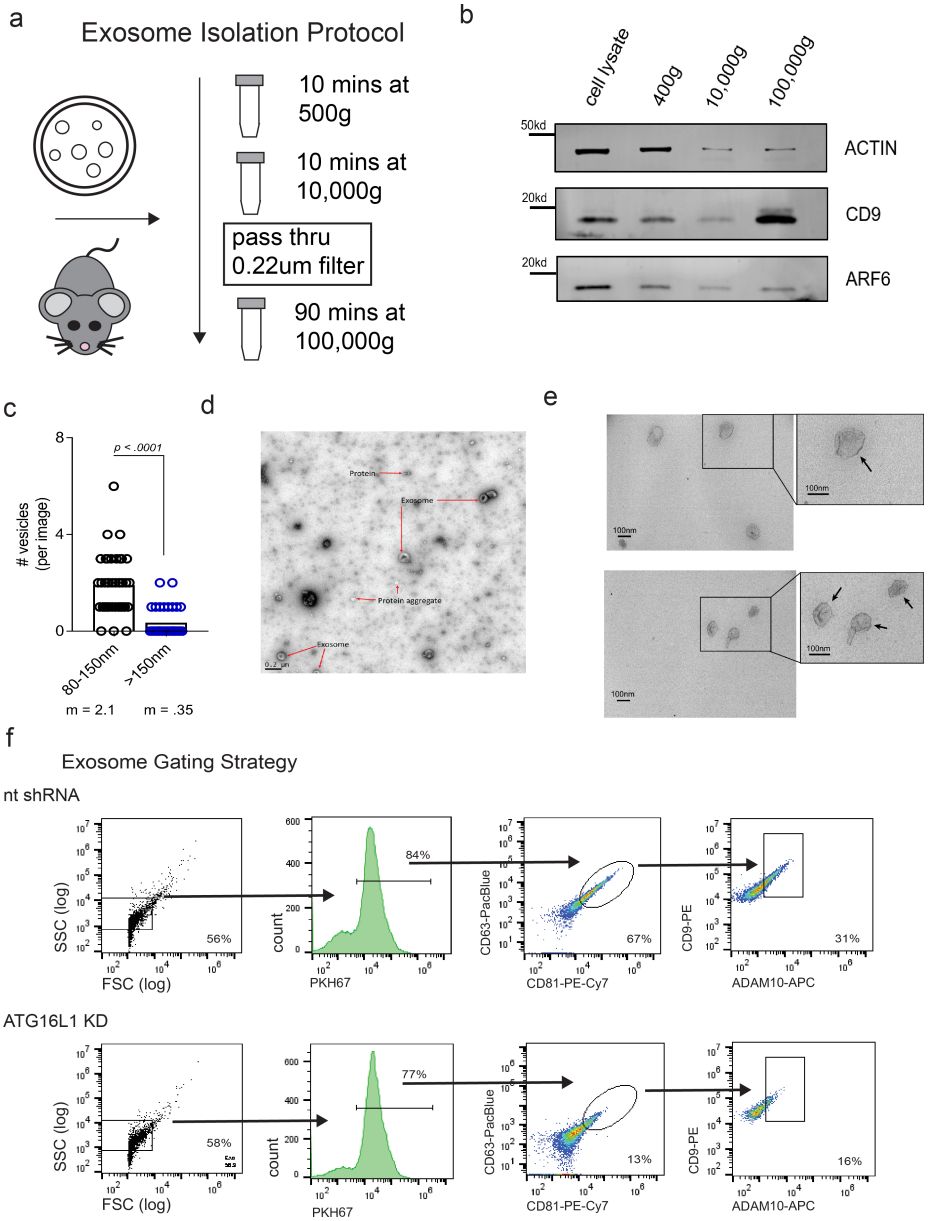

Extended Data Fig. 2 | Exosome-isolation and quantification strategies. **a**, Exosome-isolation protocol from in vitro or in vivo sources. Exosomes are isolated using a multistep centrifugation procedure including a 0.22-µm filtration step. **b**, Western blot of actin, ARF6 and CD9 following each sequential centrifugation step during exosome isolation. **c**, Electron-microscopy (EM) quantification of vesicles 80–150 nm and greater than 150 nm in size; $n = 80$ images. **d**, EM negative staining of exosome fractions. Arrows indicate exosomes and protein aggregates. **e**, Representative EM images of the exosome fraction, and zoomed insets with arrows indicating the single membranes of exosomes. **f**, Gating strategy and representative flow-cytometry plots from nt shRNA and ATG16L1 KD samples of six independently repeated experiments. Exosomes were stained with antibodies against CD9, CD63, CD81 and ADAM10. Exosomes were concurrently labelled with PKH67, a lipid-membrane-incorporating dye. FSC, forward scatter; SSC, side scatter. Measurements were taken from distinct samples and graphs show means ± s.e.m. **c**, Two-tailed, unpaired *t*-test with Welch's correction compared with PBS controls.

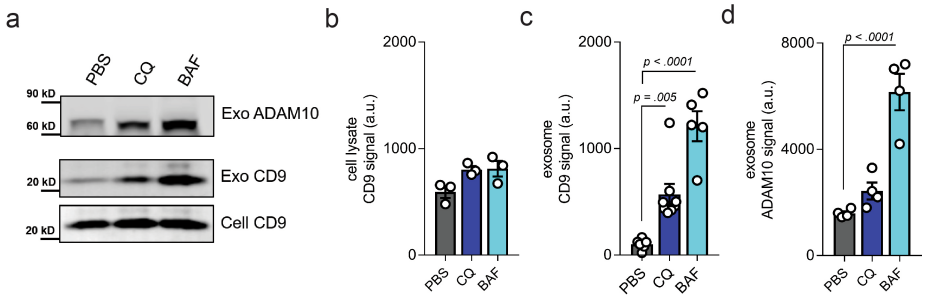

Extended Data Fig. 3 | CQ and BAF elicit production of ADAM10-positive exosomes. a–**d**, Western blot analysis of cell lysate CD9 (cell CD9), exosome CD9 (exo CD9) and exosome ADAM10 (exo ADAM10) following addition of CQ or BAF. Shown are a representative western blot from six independent experiments (**a**) and quantification of cell CD9 (**b**), exosome CD9 (**c**), and exosome ADAM10 (**d**) after PBS, CQ or BAF treatment. Measurements were taken from distinct samples, and graphs show means ± s.e.m. **b**–**d**, One-way ANOVA with Dunnet's post-test compared with PBS controls.

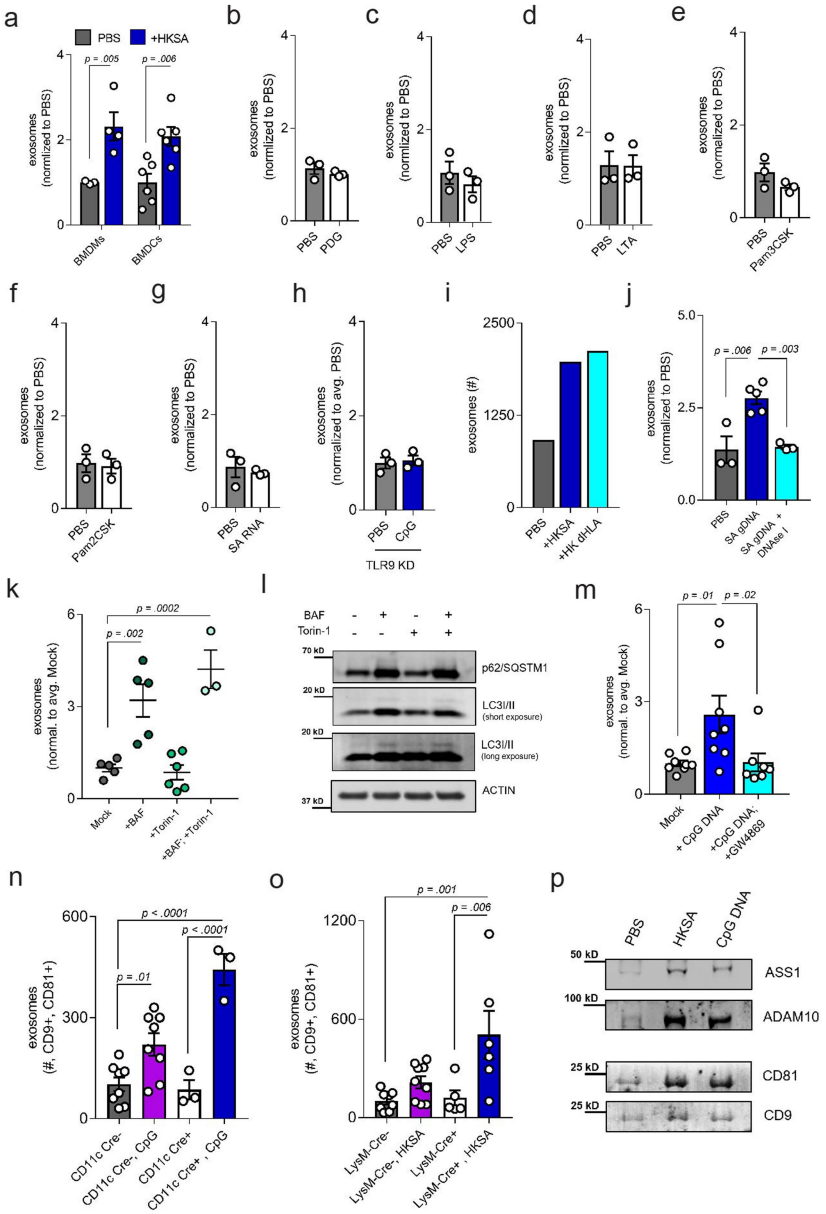

Extended Data Fig. 4 | Exosomes are produced in response to bacterial exposure. a, Flow-cytometry quantification of exosomes per 100,000 events in mouse BMDCs and BMDMs with or without exposure to HKSA (BMDCs plus PBS, $n = 6$; BMDCs plus HKSA, $n = 6$; BMDMs plus PBS, $n = 3$; BMDMs plus HKSA, $n = 4$). **b**–**h**, Quantification of total exosomes in A549 cell-culture supernatant by flow cytometry 18 h after treatment with peptidoglycan (PDG; **b**), lipopolysaccharide (LPS; **c**), lipoteichoic acid (LTA; **d**), Pam3CSK (**e**), Pam2CSK (**f**) or *S. aureus* RNA (SA RNA; **g**); $n = 3$. **h**, Quantification of total exosomes in TLR9 KD A549 cell-culture supernatants following treatment with CpG DNA; $n = 3$. **i**, Flow-cytometry quantification of A549-produced exosomes following exposure to HKSA or to a strain of *S. aureus* deficient in the production of α-toxin (HK dHLA). **j**, Flow-cytometry quantification of exosomes isolated from A549 cells treated with PBS ($n = 3$), *S. aureus* genomic DNA (SA gDNA; 0.5 μg ml^{-1}; $n = 5$), and/or DNase I ($n = 2$). **k**, Flow-cytometry quantification of exosomes isolated from cells treated with BAF ($n = 5$), Torin-1 ($n = 6$), or both ($n = 3$). **l**, Representative western blot of SQSMT1, LC3I/II and actin in cells treated with BAF, Torin-1 or both 4 h after treatment, from two independent experiments. **m**, Flow-cytometry quantification of exosomes from A549 cells treated with PBS (mock treatment; $n = 8$), CpG DNA ($n = 8$), or CpG DNA and GW4869 ($n = 7$). **n**, **o**, Plasma exosome quantification of ATG16L1 flow/flox; CD11c-Cre (**n**), and ATG16L1 flow/flox; LysM-Cre (**o**) following exposure to either CpG DNA or HKSA, respectively. **p**, Representative western blot of ADAM10, ASS1, CD9 and CD81 in exosome fractions submitted to mass spectrometry, from three independent experiments. Measurements were taken from distinct samples and graphs show means ± s.e.m. **a**, **b**–**h**, Two-tailed, unpaired *t*-test with Welch's correction compared with PBS controls. **j**, **k**, **m**–**o**, One-way ANOVA with Dunnet's post-test compared with PBS, mock, CpG DNA or Cre−/+ controls.

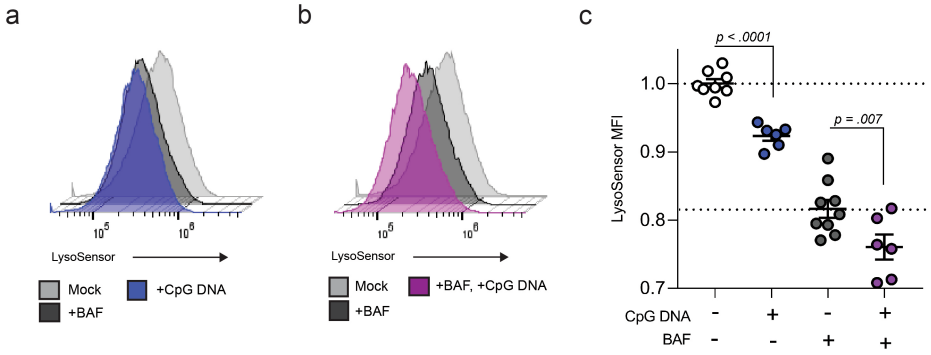

Extended Data Fig. 5 | BAF and CpG DNA decrease acidic organelles. **a**–**c**, Representative flow-cytometry histograms from three independent experiments of Lysosensor signal following treatment with BAF or CpG DNA (**a**), or BAF with or without CpG DNA (**b**). **c**, Quantification of Lysosensor MFI following treatment with PBS alone (no BAF or CpG DNA; $n = 8$), BAF ($n = 6$), CpG DNA ($n = 9$), or BAF plus CpG DNA ($n = 6$) (**c**). Measurements were taken from distinct samples and graphs show means ± s.e.m. **c**, One-way ANOVA with Dunnet's post-test compared with PBS controls.

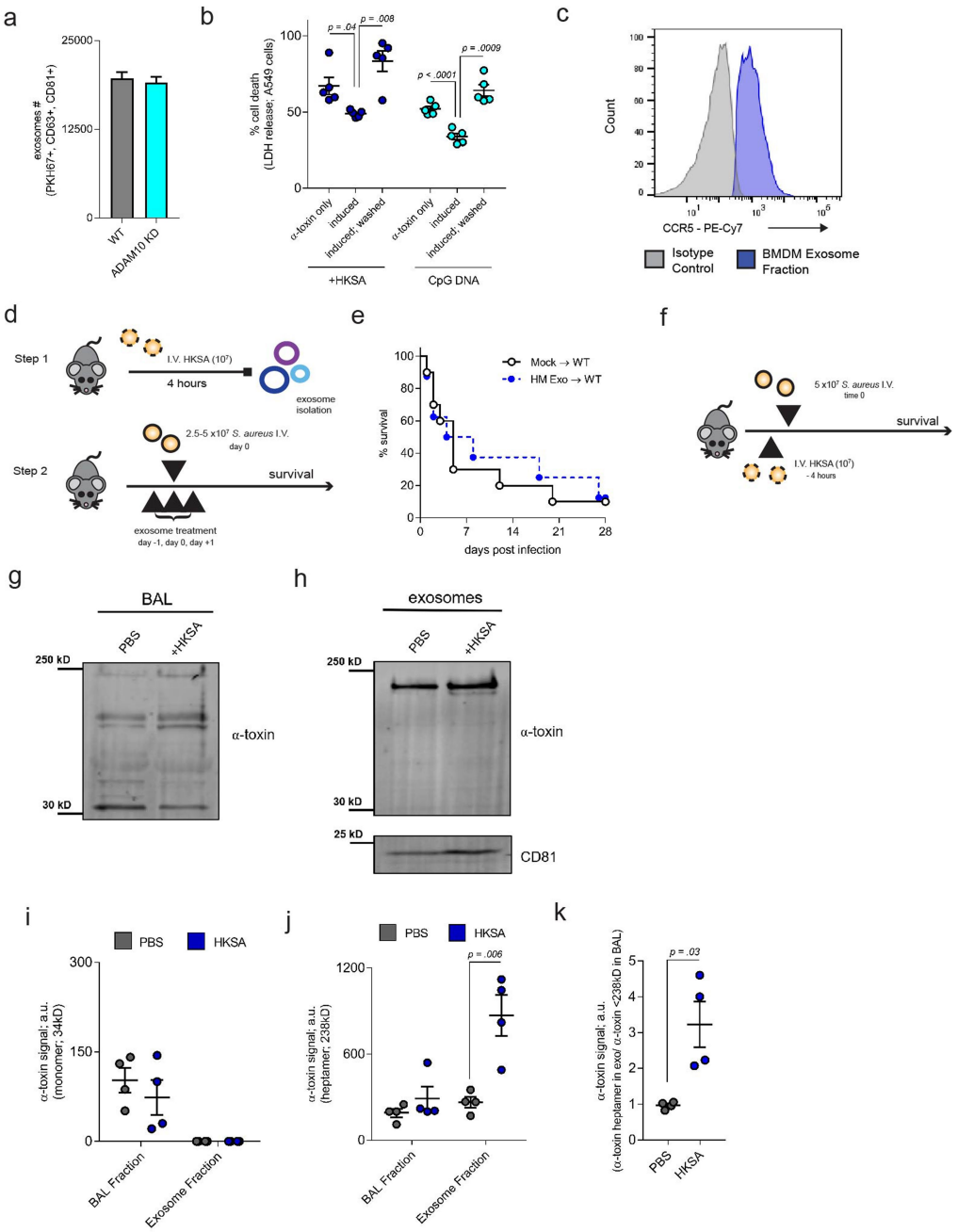

Extended Data Fig. 6 | Exosomes protect from *S. aureus* toxicity in vitro and in vivo. a, Flow-cytometry exosome quantification from nt shRNA control and ADAM10 KD A549 cells; $n = 3$. **b**, Cell death, measured by LDH release, of A549 cells treated with α-toxin only, pretreated with HKSA or CpG DNA and α-toxin ('induced'), or pre-exposed to HKSA or CpG DNA followed by PBS wash and then α-toxin treatment ('induced; washed'); $n = 5$. **c**, Representative flow-cytometry histograms of CCR5 on CD81-positive, CD63-positive and CD9-positive exosomes isolated from mouse BMDMs. **d**, Exogenous exosome-transfer protocol. In step 1, donor mice are pre-exposed to HKSA i.v. to induce exosome production. In step 2, exosomes from donor mice are injected intraperitoneally (i.p.) on day −1, day 0 and day +1 following lethal i.v. injection of *S. aureus*. **e**, Survival of wild-type mice infected i.v. with a lethal dose of 5×10^7 CFU of *S. aureus* (USA300) that were mock-treated ($n = 10$) or injected i.p. with exosomes from *Atg16l1*^{HM} mice ($n = 8$). **f**, Endogenous exosome-protection protocol. Mice are i.v. injected with HKSA to induce exosome production. Four hours later, mice are infected with a lethal dose of *S. aureus* ($2.5–5 \times 10^7$). **g**, **h**, Western blot analysis of α-toxin oligomerization in total BAL or in exosome fraction in BAL of mice pre-exposed to HKSA or PBS intranasally (i.n.), representative of four independent experiments. **i**, **j**, Quantification of α-toxin monomer (**i**) and heptamer (**j**) in BAL and exosome fraction following pre-exposure; $n = 4$. **k**, Ratio of α-toxin heptamer in exosome fraction to total α-toxin signal in BAL; $n = 4$. Measurements were taken from distinct samples and graphs show means ± s.e.m. **a**, **i**–**k**, Two-tailed, unpaired *t*-test with Welch's correction. **b**, One-way ANOVA with Dunnet's post-test compared with α-toxin only or 'induced' controls. **e**, log-rank Mantel–Cox test.

nature research

Corresponding author(s): Ken Cadwell

Reporting Summary

Nature Research wishes to improve the reproducibility of the work that we publish. This form provides structure for consistency and transparency in reporting. For further information on Nature Research policies, see Authors & Referees and the Editorial Policy Checklist.

Statistical parameters

When statistical analyses are reported, confirm that the following items are present in the relevant location (e.g. figure legend, table legend, main text, or Methods section).

n/a	Confirmed	
☐	☒	The exact sample size (*n*) for each experimental group/condition, given as a discrete number and unit of measurement
☐	☒	An indication of whether measurements were taken from distinct samples or whether the same sample was measured repeatedly
☐	☒	The statistical test(s) used AND whether they are one- or two-sided *Only common tests should be described solely by name; describe more complex techniques in the Methods section.*
☐	☒	A description of all covariates tested
☐	☒	A description of any assumptions or corrections, such as tests of normality and adjustment for multiple comparisons
☐	☒	A full description of the statistics including central tendency (e.g. means) or other basic estimates (e.g. regression coefficient) AND variation (e.g. standard deviation) or associated estimates of uncertainty (e.g. confidence intervals)
☐	☒	For null hypothesis testing, the test statistic (e.g. *F*, *t*, *r*) with confidence intervals, effect sizes, degrees of freedom and *P* value noted *Give P values as exact values whenever suitable.*
☒	☐	For Bayesian analysis, information on the choice of priors and Markov chain Monte Carlo settings
☒	☐	For hierarchical and complex designs, identification of the appropriate level for tests and full reporting of outcomes
☐	☒	Estimates of effect sizes (e.g. Cohen's *d*, Pearson's *r*), indicating how they were calculated
☐	☒	Clearly defined error bars *State explicitly what error bars represent (e.g. SD, SE, CI)*

Our web collection on statistics for biologists may be useful.

Software and code

Policy information about availability of computer code

Data collection	Flow cytometry data was collected and performed on a Beckman Coulter CytoFlex S. Western blots were imaged and analyzed using the Li-COR Odyssey Clx.
Data analysis	All data was analyzed using Graphpad Prism v7. FlowJo v 10 was used to analyze all flow cytometry experiments. Western blots were analyzed using the Li-COR Odyssey Image Studio Ver 5.2. Genewiz was used to evaluate and confirm colony PCR and sequencing data. Mass spectrometry data was analyzed using Proteome Discoverer 1.4 .

For manuscripts utilizing custom algorithms or software that are central to the research but not yet described in published literature, software must be made available to editors/reviewers upon request. We strongly encourage code deposition in a community repository (e.g. GitHub). See the Nature Research guidelines for submitting code & software for further information.

Data

Policy information about availability of data

All manuscripts must include a data availability statement. This statement should provide the following information, where applicable:

- Accession codes, unique identifiers, or web links for publicly available datasets
- A list of figures that have associated raw data
- A description of any restrictions on data availability

Authors can confirm that all relevant data are included in the paper and/or its supplementary information files

Field-specific reporting

Please select the best fit for your research. If you are not sure, read the appropriate sections before making your selection.

☒ Life sciences ☐ Behavioural & social sciences ☐ Ecological, evolutionary & environmental sciences

For a reference copy of the document with all sections, see nature.com/authors/policies/ReportingSummary-flat.pdf

Life sciences study design

All studies must disclose on these points even when the disclosure is negative.

Sample size	The number of animals used in the experiments in this study is estimated based on a power analysis with the following assumptions: standard deviation will be ~20% of the mean, p-value will be under 0.05 when the null hypothesis is false, the effect size (Cohen's d) is between 1.0-2.0. The minimal number of mice required under these conditions ranges between 6-28 for in vivo experiments. Additionally, we have carefully chosen the sample size listed below based on empirical evidence of what is necessary for interpretation of the data and statistical significance.
Data exclusions	No data was excluded from the analysis.
Replication	In all experiments reported, each cell culture and animal experiment was attempted at least two times. In all experiments, no attempts at replication failed.
Randomization	Groups were established based off genotype and infection status. All other aspects were randomized.
Blinding	Investigator blinding was not used or necessary in this study as no quantification of subtle data or phenotypes were required.

Reporting for specific materials, systems and methods

Materials & experimental systems

n/a	Involved in the study
☐	☒ Unique biological materials
☐	☒ Antibodies
☐	☒ Eukaryotic cell lines
☒	☐ Palaeontology
☐	☒ Animals and other organisms
☒	☐ Human research participants

Methods

n/a	Involved in the study
☒	☐ ChIP-seq
☐	☒ Flow cytometry
☒	☐ MRI-based neuroimaging

Unique biological materials

Policy information about availability of materials

Obtaining unique materials	All unique materials used are readily available from the authors.

Antibodies

Antibodies used	Flow: CCR5 (mouse HM-CCR5, 1:200), EpCAM (human, 9C4, 1:500), CD81 (human, 5a6; mouse, Eat-2, 1:200), CD9 (human, HI9a; mouse, MZ3, 1:200), CD63 (human, H5C6; mouse, NVG-2, 1:200), ADAM10 (human, SHM14, 1:200) all purchased from BioLegend. Western Blot: CD9 (Cat# 13174S, Cell Signaling, 1:1000), CD81 (cat# ab109201, Abcam, 1:1000), ADAM10 (Cat#

	AB19026, Millipore, 1:2500), LC3 (Cat# PM026, MBL, 1:1000), SQSTM1 (Cat# P0067, Sigma, 1:4000), HLA/a-toxin (Cat# S75531, Sigma, 1:5000), ACTIN (Cat# A5441, Sigma, 1:10,000), STX17 (Cat# NBP1-93968, Novus Biologicals, 1:2500), ARF6 (Cat# 5740S, Cell Signaling, 1:1000), ASS1 (Cat# ab124465, Abcam, 1:1000).
Validation	All reported commercial antibody validation can be found on vendor websites.

Eukaryotic cell lines

Policy information about cell lines

Cell line source(s)	Human lung epithelial purchased from ATCC (A549), and human embryonal kidney cells (293FT, ThermoFisher cat#R70007) were used for lentiviral packaging.
Authentication	ATCC Cell Line Authentication, Service Sanger Sequencing
Mycoplasma contamination	Confirmed negative for mycoplasm
Commonly misidentified lines (See ICLAC register)	No commonly misidentified cell lines were used.

Animals and other organisms

Policy information about studies involving animals; ARRIVE guidelines recommended for reporting animal research

Laboratory animals	This study uses mice from the wildtype (WT) and Atg16L1 hypomorph on the C57BL/6 background. Both male and female mice approximately 8-10 weeks of age are used.
Wild animals	Study does not involve wild animals.
Field-collected samples	Study does not involve field-collected samples.

Flow Cytometry

Plots

Confirm that:

☒ The axis labels state the marker and fluorochrome used (e.g. CD4-FITC).

☒ The axis scales are clearly visible. Include numbers along axes only for bottom left plot of group (a 'group' is an analysis of identical markers).

☒ All plots are contour plots with outliers or pseudocolor plots.

☒ A numerical value for number of cells or percentage (with statistics) is provided.

Methodology

Sample preparation	Exosomes were collected from culture supernatants or plasma via high speed centrifugation prior to staining with flow cytomtery antibodies (as described in manuscript). Cells isolated from in vitro assays were removed using 5mM EDTA and washed in PBS containing FBS prior to staining.
Instrument	Beckman Coulter CytoFlex S
Software	Flow data was collected with BD CytExpert Software and analyzed using FloJo v 10.
Cell population abundance	In sorting experiment, purity of samples was determined at the time of sorting by running a sorted sample on the FACSAria. All samples tested were more than 95% pure.
Gating strategy	Cells were gated on FCS-A and SSC-A. Doublets were removed by gating FSC-A v FSC-H. Live cells were gated as Zombie-Dye negative. Cells were then gated on for ADAM10 or EpCAM. Exosomes were gated as PKH67+CD81+CD63+CD9+. Exosomes were also stained with ADAM10 unless otherwise mentioned. All gates were set using an antibody isotype control samples.

☒ Tick this box to confirm that a figure exemplifying the gating strategy is provided in the Supplementary Information.